TRENDS IN SCIENCES 2025; 22(11): 10678
https://doi.org/10.48048/tis.2025.10678
RESEARCH ARTICLE

Salacca zalacca Skin as a Potential Adjuvant for Metabolic Syndrome Therapy: Integrative *In Vitro* and Computational Approaches

Diana Yuswanti Putri[1], Yuyun Yueniwati[2,*], Sri Utami[1], Mokhamad Fahmi Rizki Syaban[3], Nirmala Halid[4], Purnawan Pontana Putra[5], Sastia Prama Putri[6] and Husnul Khotimah[3]

[1]*Doctoral Program in Medical Sciences, Faculty of Medicine, Universitas Brawijaya, East Java 65145, Indonesia*
[2]*Department of Radiology, Faculty of Medicine Universitas Brawijaya, Saiful Anwar General Hospital, East Java 65111, Indonesia*
[3]*Faculty of Medicine, Universitas Brawijaya, East Java 65145, Indonesia*
[4]*Master Program in Biomedical Science, Faculty of Medicine Universitas Brawijaya, East Java 65145, Indonesia*
[5]*Department of Pharmaceutical Chemistry, Faculty of Pharmacy, Universitas Andalas, Padang 25163, Indonesia*
[6]*Department of Biotechnology, The University of Osaka, Osaka 565-0871, Japan*

([*]Corresponding author's e-mail: yuyun@ub.ac.id)

Received: 17 May 2025, Revised: 24 June 2025, Accepted: 10 July 2025, Published: 20 August 2025

Abstract

Metabolic syndrome (MetS) remains a health concern condition characterized by hyperglycemia, obesity, and hypertension, requiring effective interventions such as antioxidant support and inhibition of digestive enzymes. *Salacca zalacca* skin (SZS), traditionally used for its antioxidant, anti-inflammatory, and lipid-lowering properties, shows promise in addressing MetS, though its molecular mechanisms remain underexplored. This study evaluated the potential of ethanol extract of SZS in managing MetS through *in vitro* and *in silico* approaches. LC-MS/MS analysis identified 16 bioactive compounds. Network pharmacology and molecular docking revealed that diphyllin, 19-norandosterone, and anastrozole exhibited strong and stable binding affinities to MetS-related targets: TNF-α (−6.7, –6.6, and –6.1 kcal/mol) and PPARG (−7.4, –7.1, and –7.9 kcal/mol), supported by molecular dynamics simulations. Antioxidant assays demonstrated moderate activity, with EC_{50} values of 776.4 µg/mL (ABTS) and 647.8 µg/mL (DPPH). SZS inhibited lipase (EC_{50} = 4,330 µg/mL) and α-glucosidase (EC_{50} = 481.1 µg/mL), indicating its potential to regulate lipid and glucose metabolism.

These findings suggest that SZS may exert multi-targeted effects by scavenging free radicals, inhibiting digestive enzymes, and modulating inflammatory and metabolic pathways. This study is the 1st to integrate *in vitro* and *in silico* evidence for SZS in MetS management, laying the groundwork for its development as a nutraceutical. Future research should focus on formulation refinement, compound synergy, and long-term clinical validation.

Keywords: *Salacca zalacca* skin; Metabolic syndrome; Metabolomic; *in vitro*; *in silico*.

Introduction

Metabolic syndrome (MetS) is defined by a cluster of metabolic abnormalities, including abdominal obesity, dyslipidemia, hypertension, and hyperglycemia, which significantly contribute to its development and progression [1]. MetS imposes a substantial health and economic burden worldwide, with its prevalence steadily increasing [2,3]. It begin form chronic hyperglycemia impairs insulin function and increases oxidative stress, contributing to the development of metabolic syndrome (MetS). Digestive enzymes like α-glucosidase break down carbohydrates into monosaccharides, causing a spike in post-prandial blood glucose [4]. Obesity and high fat intake also worsen MetS by increasing lipase activity, which breaks down triglycerides into monoglycerides, glyceryl esters and free fatty acids, further disrupting insulin function [5]. MetS is closely linked to chronic inflammation and oxidative stress. One key contributor is tumor necrosis

factor-α (TNF-α), a pro-inflammatory cytokine involved in obesity and believed to play a role in obesity-related metabolic disorders [6]. Additionally, modulation of peroxisome proliferator-activated receptor gamma (PPARG) is crucial in the regulation and treatment of MetS [7].

Lifestyle modifications improve this condition but have a low compliance rate [8]. Statins, ACE inhibitors, metformin, and canagliflozin are commonly used to manage metabolic syndrome (MetS). However, the rising prevalence of MetS and obesity indicates that current therapies may be insufficient, highlighting the need for effective adjuvant options [9]. Natural products offer a promising and safer alternative. Moreover, *in silico* and *in vitro* approaches enable the rapid screening of bioactive compounds, supporting the development of complementary and sustainable treatment strategies. To overcome the limitations of current therapies, natural products such as *Salacca zalacca* skin (SZS) are promising potential adjuvants to help control MetS. Various *Salacca zalacca* skin (SZS) variants contain beneficial compounds such as alkaloids, steroids, triterpenoids, flavonoids, and tannins [10]. These bioactive components offer a range of health benefits, including anti-aging effects [10], potential use in natural cosmetics [11], and antidiabetic properties [12]. This study aims to investigate the potential of SZS as an adjuvant agent for the management of metabolic syndrome (MetS) that may enhance the effectiveness of existing treatments. Identifying natural bioactive compounds through *in vitro* and computational studies may contribute to the development of safer and more effective complementary treatment strategies.

Materials and methods

This study started by extracting SZS with 96% ethanol, followed by non-target compound screening. Two analytical approaches were applied: *in silico* prediction of compound interactions with MetS-related proteins, and *in vitro* evaluation of the extract's antioxidant and digestive enzyme inhibitory activities. This serves as a key initial step toward developing nutraceuticals and adjuvant therapies.

Chemical and reagents

ABTS diammonium salt (AzBTS-(NH4)2) (cat. no. GC33439), α-glucosidase (cat. no. GC63270), acarbose (cat. no. GC10751), orlistat (cat. no. GC17318), α-amylase (cat. no. GC19359), and Trolox (cat. no. GC19457) were purchased from GLPBIO (Montclair, CA, USA). DMSO (cat. no. 786-1323) was obtained from G-Bioscience (Indonesia), while 1,1-diphenyl-2-picrylhydrazyl free radical (cat. no. D4313-1G) and 3,5-dinitrosalicylic acid (cat. no. D0850-100G) were procured from TCI (Tokyo, Japan). Potassium persulfate (cat. no. P823296), 4-Nitrophenyl butyrate (cat. no. N832938), 4-Nitrophenyl α-D-glucopyranoside (cat. no. N814753), and lipase (cat. no. L812480) were acquired from MACKLIN (Pudong, Shanghai).

Samples extraction

The *Salacca zalacca* skin (SZS) was sourced from *salak pondoh* fruit Pronojiwo cultivar, Lumajang Regency, East Java, Indonesia. The plant identification was carried out at Materia Medica, Batu, East Java, Indonesia. The extraction process involved macerating 200 g of SZS simplicial powder in 2 liters of 96% ethanol for 5 days (5×24 h). The filtration was performed using Whatman No. 42 (125 mm) paper to separate the soluble fraction, which was subsequently evaporated using a rotatory evaporator at 90 °C for 40 - 60 min. The resulting extract was dried in the oven at 70 °C for 2 days before further assay (see **Figure 1**).

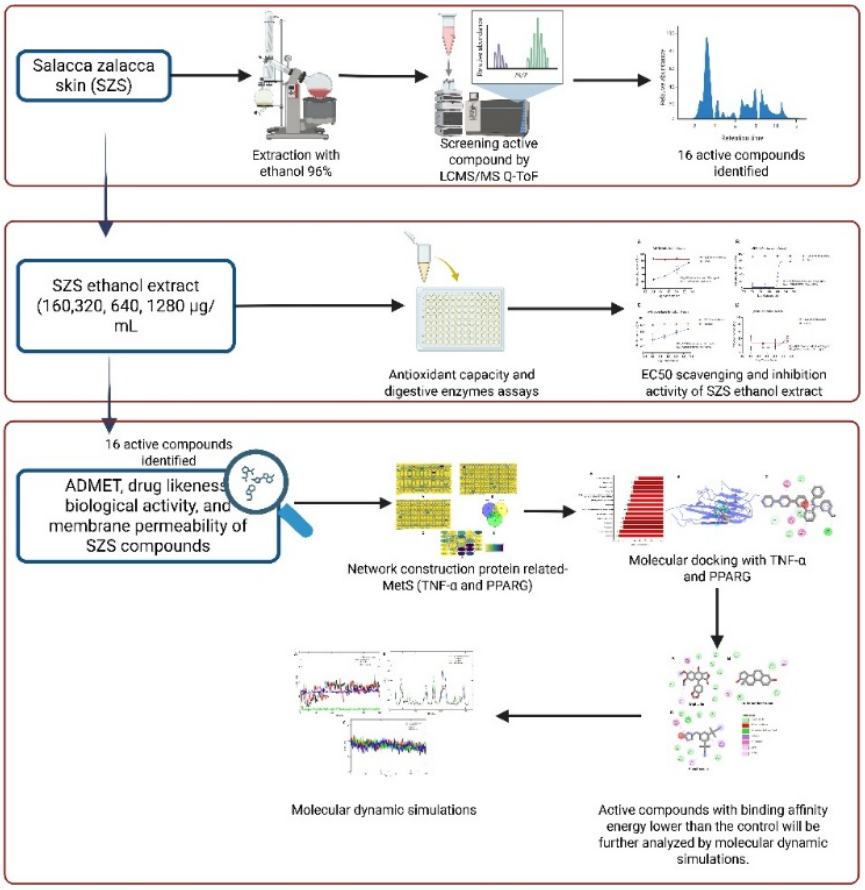

Figure 1 Graphical workflow overview.

Metabolomic profiling through LCMS/MS Q-ToF

The identification of the ethanol extract of SZS conducted using mass spectrometry (Xevo G2-S QTof, Waters, USA) at a column temperature of 50 °C and room temperature of 25 °C. The liquid chromatography (LC) was conducted using a mobile phase consisting of water + ammonium formic and acetonitrile + 0.05% formic acid, with a flow rate of 0.2 mL/min for 23 min and an injection volume of 5 µL. The mass spectrometry (MS) analysis was carried out using electrospray ionization (ESI) in positive mode with a mass range of 50 - 1,200 m/z. The source and desolvation temperatures were set to 100 and 350 °C, respectively. The analysis of phytocompounds was carried out using LCMS-MS/Q-ToF in Masslynx software (version 4.1), which contains a library of mass spectra of compounds and allows the identification of the mass spectra of compounds in the sample.

ADMET and drug-likeness of SZS

The absorption, distribution, metabolism, excretion, and toxicity (ADMET) properties of the SZS phytocompounds were evaluated using SwissADME (http://www.swissadme.ch/) [13,14]. Lipinski's Rule of 5 (LR5) was applied to evaluate the ideal drug candidates, typically have no more than 5 hydrogen bond donors, no more than ten hydrogen bond acceptors, a molecular weight under 500 Da, and a partition coefficient (log P) of 5 or less [14,15].

Biological activity and permeability of molecules prediction

The biological activity of active compounds in SZS was predicted using the Prediction of Activity Spectra for Substances (PASS) online web server (http://www.way2drug.com/index.php) [16] and then visualized using GraphPad Prism software version 10 (https://www.graphpad.com/features). Then, the passive permeability across lipid bilayers was assessed using the Permeability Molecules Across Membranes (perMM) online web server (https://permm.phar.umich.edu/) [17]

and visualized using ChimeraX (https://www.cgl.ucsf.edu/chimerax/) [18].

Network construction of MetS

Genes associated with metabolic syndrome (MetS) were identified using 3 databases: NCBI (https://www.ncbi.nlm.nih.gov/gene/), DisGENET (https://www.disgenet.org/), and GeneCards (https://www.genecards.org/), with the keyword "metabolic syndrome" and restricted to human (Homo sapiens) genes. The overlapping genes were found using Venny 2.1 (https://bioinfogp.cnb.csic.es/tools/venny/) and imported into Cytoscape 3.10.0 to build a Target-Disease network. The network was analyzed using Cytoscape's built-in tools, and key target genes were identified using the CytoCluster plug-in [19].

Molecular docking

In this study, molecular docking simulations were conducted using TNF-α and PPARG as target proteins (PDB IDs: 5MU8 and 2PRG). Phytocompounds from SZS were downloaded from PubChem (https://pubchem.ncbi.nlm.nih.gov/compound/) and prepared using the PyRx (https://pyrx.sourceforge.io/) program with AutoDock Vina on a personal computer (Lenovo IdeaPad Slim 3, Intel core i3 (10^{th} generation), 8 GB RAM, Windows 11 operating system). Protein structures were processed by removing water molecules and native ligands using Discovery Studio 2021. The compounds were converted from SDF format, energy-minimized, and docked to the proteins by defining grid coordinates (Supplementar**y Table 1**). Docking results were saved and visualized using Discovery Studio. To confirm accuracy, a redocking process was performed (RMSD values required to be <2.0 Å) [20]. Docking and grid parameters were adjusted based on these validations [21-23].

Molecular dynamics simulation

Protein topologies were generated with the AMBER99SB-ILDN force field using pdb2gmx, and ligand topologies were prepared using Acpype to ensures accurate simulation of protein-ligand interactions. The system was neutralized with NaCl at physiological pH and used periodic boundary conditions. Long-range electrostatics were calculated using the Particle-Mesh Ewald (PME) method, with Fast Fourier Transform (FFT) used computational efficiency, and the TIP3P water model was used for solvation. Simulations began with energy minimization, followed by equilibration under NVT (250 ps) and NPT (250 ps) conditions. The main production run was performed for 100 ns under NPT conditions at 310 K using GROMACS 2024.1 [24]. Binding free energies were calculated across simulation frames using UNI-GBSA [25] and gmx-MMPBSA [26].

DPPH scavenging radical assessment

For the DPPH assay, a 0.4 mM DPPH solution was prepared by dissolving 10 mg of DPPH in 25 mL of ethanol in a volumetric flask lined with aluminum foil. This solution was used to test DPPH scavenging at the same time. The SZS ethanol extract was diluted to concentrations ranging from 160, 320, 640, and 1,280 µg/mL. Each well received 100 µL of the extract and 100 µL of the DPPH solution. The plates were then incubated at room temperature for 30 min, and absorbance readings were taken at 517 nm using a microplate reader [27]. The same procedure was performed on control Trolox. To ensure accuracy and reliability, the test was performed in triplicate (n = 3). The inhibitions percentages were calculated using the appropriate formulas as follows:

$$\text{Scavenging activity (\%)} = \frac{\text{Absorbance}_{\text{control}} - \text{Absorbance}_{\text{reaction}}}{\text{Absorbance}_{\text{control}}} \times 100$$

ABTS scavenging radical assessment

The ABTS antioxidant assay was carried out according to the procedure described by Nurkolis et al. with modifications [28]. Briefly, the 7 mM ABTS solution was prepared by dissolving 8 mg of ABTS powder in 1 mL of distilled water. Separately, a 2.45 mM potassium persulfate solution was made by dissolving 13.2 mg of potassium persulfate in 10 mL of distilled water. These 2 solutions were mixed in a 1:1 ratio in a volumetric flask, covered with aluminum foil, and incubated at room temperature in the dark for 12 - 16 h. The absorbance of the solution was adjusted to 0.0706 at 734 nm by adding 50% ethanol. A 96% ethanol blank was used as the absorbance control. Various concentrations of SZS ethanol extract (160, 320, 640 and 1,280 µg/mL) were prepared, along with the control drug Trolox to test the antioxidant activity.

Tests were performed in 96-well plates, with 100 µL of the extract and 200 µL of ABTS reagent added to each well. The wells were then incubated at 37 °C for 15 min, and absorbance readings were taken at 734 nm using a microplate reader. The same procedure was carried out for control Trolox.

Glucosidase inhibition assay

The α-glucosidase inhibition assay was conducted using a colorimetric assay in 96-well plates, following the protocol of Unuofin *et al.* [29] with modifications. Each well received 40 µL α-glucosidase solution (1 U/mL) and 20 µL of the SZS ethanol extract at various concentrations (160, 320, 640, and 1,280 µg/mL) and acarbose as a control. The mixture was incubated at 37 °C for 5 min. Subsequently, 10 µL of PNP-GLUC (4 mM) was added to initiate the reactions, followed by a 2nd incubation at 37 °C for 30 min. The reaction was terminated by adding 100 µL of sodium carbonate (1M) to each well, and the absorbance was measured at of 405 nm using a microplate reader. Each test was performed in triplicate (n = 3) to ensure the reliability and accuracy of the results.

Lipase inhibition assay

Pancreatic lipase (2 mg/mL) was dissolved in phosphate buffer (50 mM, pH 7.0) and centrifuged at 12,000 g to remove insoluble components. A 20 µL extract at varying concentrations (160, 320, 640, and 1,280 µg/mL) was mixed with 80 µL of lipase enzyme. The mixture was incubated at 37 °C for 15 min. Subsequently, 170 µL (1M) of p-nitrophenyl butyrate (pNPB) was added to each well, and the reaction was allowed to proceed for 25 min at 37 °C. Absorbance was measured at 405 nm using a microplate reader. All experiments were conducted in triplicate (n = 3) to ensure the reliability of the results [30]. The same procedure was carried out for control orlistat.

Data analysis

The statistical analysis was performed using GraphPad Prism software version 10 (https://www.graphpad.com/features). Each concentration of the extract and control was converted to log10, and nonlinear regression analysis "log(inhibitor) vs. normalised response-variable slope)" was performed to determine the half-maximal effective concentration (EC50). The visualization was performed graphically using GraphPad Prism version 10 (https://www.graphpad.com/features).

Results and discussion

Metabolomic profiling

Metabolic profiling is a comprehensive analytical approach that provides precise information about the compounds contained in a natural product. This method plays a crucial role in elucidating specific metabolic pathways, identifying disease biomarkers, and evaluating the impact of environmental or pharmacological factors on metabolism [31,32]. To investigate the metabolite composition of SZS ethanol extract, a non-targeted metabolomic profiling approach was employed using liquid chromatography–mass spectrometry (LC-MS/MS) with a high-resolution quadrupole time-of-flight (Q-ToF) instrument. Electrospray ionization (ESI) was performed in positive mode, covering a mass-to-charge (m/z) range of 50 - 1,200, with a total run time of 23 min. The retention time refers to the time at which each compound is detected by the instrument, as depicted in Supplementary **Figure 1**.

This analysis successfully identified 16 active compounds (Supplementary **Table 2**), representing several important phytochemical classes. These included phenols (e.g., butyl salicylic acid), glycosides (e.g., citrusic E, hydroxytyrosol 3′-glucuronide), fatty acids (e.g., calendic acid - a form of linoleic acid), terpenoids (e.g., 2-deacetoxy taxinine B), and other compounds such as metyrapol, a pyridine derivative. Each of these classes is associated with well-documented biological functions. Phenolic compounds act as potent antioxidants and contribute to plant defense mechanisms against ultraviolet radiation and microbial attack, while also playing a role in the prevention of oxidative stress-related diseases in humans [33,34]. Glycosides, which consist of sugar moieties linked to non-sugar aglycones, are known for a wide range of therapeutic effects, including cardioprotective, antidiabetic, anticancer, and antioxidant properties [35-37]. Calendic acid, an essential polyunsaturated fatty acid, supports skin integrity, neurological development, and serves as a precursor to arachidonic acid, which is vital for fetal and infant brain growth [38].

Metabolomic analysis via LC-MS/MS Q-Tof is the 1st method conducted in SZS screening. Previous phytochemical investigations have confirmed the presence of phenolic compounds, tannins, flavonoids, alkaloids, saponins, and triterpenoids in snake fruit peel extracts [39,40]. For instance, Girsang *et al.* [39] used LC-ESI-MS to screen for specific compounds and detected chlorogenic acid at a concentration of 1.073 mg/g dry weight, while other expected compounds such as rutin and caffeic acid were not identified. In another study on the Sumalee cultivar from Thailand, HPLC analysis revealed the presence of multiple phenolic acids, including gallic acid, chlorogenic acid, ferulic acid, and quercetin [11].

The differences between the metabolite profiles observed in the current study and those reported previously can be attributed to several important factors. The analytical methodology employed in this study involved non-targeted LC-MS/MS-based profiling with high-resolution Q-ToF technology, which offers superior sensitivity and the capability to detect a broader spectrum of metabolites compared to the more targeted HPLC or biochemical assays used in earlier research [41]. This approach enables the identification of both known and novel compounds, including those present in low abundance [42]. The variations in extraction protocols, such as the use of 70% ethanol in the present study, likely influenced the types and quantities of compounds extracted [43]. Solvent polarity plays a critical role in determining which classes of metabolites are solubilized, with previous studies using different solvent systems that may have selectively enriched or excluded certain compound types [44].

The differences in plant material sources and varieties may significantly influence metabolite profiles. The phytochemical composition of SZS can vary based on cultivar (e.g., Medan vs. Sumalee), geographic origin, environmental conditions, and harvest timing. These biological and ecological variables affect the synthesis and accumulation of secondary metabolites in the plant [45]. The sensitivity of detection methods and the use of updated compound libraries in this study likely contributed to the identification of compounds not previously reported, such as Anastrozole and 2-Deacetoxy taxinine B. Such compounds may have been overlooked in earlier studies due to limitations in detection thresholds or the absence of comprehensive reference databases. In addition, the scope and objective of the study also play a role; whereas prior investigations focused primarily on detecting specific known compounds such as chlorogenic acid or rutin, this study aimed to obtain a complete metabolomic profile, allowing for the discovery of a more diverse range of metabolites.

ADMET and drug-likeness of SZS.

Absorption, distribution, metabolism, excretion, and toxicity (ADMET) analysis is a critical step in the early stages of drug discovery and development, as it evaluates the pharmacokinetic and toxicological properties of potential drug candidates. Using the SwissADME database [46,47], summarized in **Table 1**, revealed that most compounds demonstrated acceptable pharmacokinetic characteristics. However, Hydroxytyrosol 3'-glucuronide, Calendic acid, and 2-Deacetoxy taxinine B did not meet Lipinski's Rule of 5, suggesting limitations in their potential as orally administered therapeutic agents (**Figure 2(A)**).

Table 1 Predicted ADMET and toxicity properties of SZS compounds.

SZS compounds	Pharmacokinetic Test			Toxicity Computation Analysis					
	Water solubility	Human intestine absorption ion (HIA)	Penetrate Blood Brain Barrier (BBB)	AMES toxicity	hERG I inhibitor	hERG II inhibitor	Hepato-toxicity	Skin sensitization	T.Pyriformis toxicity
Diphyllin	Low	High	Low	Yes	No	Yes	No	No	Toxic
Anastrozole	Low	High	Low	Yes	No	No	Yes	No	Non-toxic
DL-Ornithino-L-alanine	Low	Low	Low	No	No	No	No	No	Toxic

SZS compounds	Pharmacokinetic Test			Toxicity Computation Analysis					
	Water solubility	Human intestine absorption ion (HIA)	Penetrate Blood Brain Barrier (BBB)	AMES toxicity	hERG I inhibitor	hERG II inhibitor	Hepato-toxicity	Skin sensitization	T.Pyriformis toxicity
Butyl salicylic acid	Low	High	High	No	No	No	No	No	Non-toxic
Portuloside A	Low	Medium	Low	No	No	No	No	No	toxic
Hydroxytyrosol 3'-glucuronide	Low	Low	High	No	No	No	Yes	No	Toxic
4-Hydroxy-3-prenylbenzoic acid glucoside	Low	Low	Low	No	No	No	Yes	No	Toxic
Citrusin E	Low	Medium	Low	No	No	No	Yes	No	Toxic
1,1'-(Tetrahydro-6a-hydroxy-2,3a,5-trimethylfuro[2,3-d]-1,3-dioxole-2,5-diyl)bis-ethanone	Low	High	Low	Yes	No	No	No	No	Toxic
O-Acetylcyclocalopin A	Low	Medium	Low	Yes	No	No	No	No	Toxic
Methyl (R)-9-hydroxy-10-undecene-5,7-diynoate glucoside	Low	Medium	Low	Yes	No	No	No	No	Toxic
Metyrapol	Low	High	High	No	No	No	No	No	Toxic
4-hydroxysphinganine	Low	High	Low	No	No	Yes	No	Yes	Toxic
Calendic acid	Low	High	Low	No	No	No	Yes	Yes	Toxic
19-Norandrosterone	Low	High	Medium	No	No	Yes	No	Yes	Non-toxic
2-Deacetoxy taxinine B	Low	High	Low	No	No	No	No	No	Toxic

To predict the safety of *Salacca zalacca* skin compounds, computational toxicity assessments were conducted using various models, including Ames mutagenicity, hERG I/II inhibition, hepatotoxicity, skin sensitization, and *Tetrahymena pyriformis* toxicity. The Ames test predicts mutagenic potential, serving as a preliminary screen for carcinogenicity [48], while hERG inhibition is associated with cardiac risks like long QT syndrome [49,50]. Hepatotoxicity and skin sensitization indicate risks of liver injury and allergic reactions [51,52], and *T. pyriformis* toxicity serves as a sensitive model organism for evaluating the ecological toxicity of bioactive compounds [53].

The toxicity screening results (**Table 1**) revealed that compounds Diphyllin, Anastrozole, 1,1'-(Tetrahydro-6a-hydroxy-2,3a,5-trimethylfuro[2,3-d]-1,3-dioxole-2,5-diyl)bis-ethanone, O-Acetylcyclocalopin A, and Methyl (R)-9-hydroxy-10-undecene-5,7-diynoate glucoside were predicted to be mutagenic based on the Ames test. hERG II inhibition, which contributes to cardiac risk, was predicted for Diphyllin, 4-hydroxysphinganine, and 19-Norandrosterone. Hepatotoxic potential was observed in Anastrozole, Hydroxytyrosol 3'-glucuronide, 4-Hydroxy-3-prenylbenzoic acid glucoside, Citrusin E, and Calendic acid, indicating the need for caution in considering these compounds for systemic use. Additionally, skin sensitization predictions identified 4-hydroxysphinganine, Calendic acid, and 19-Norandrosterone as likely irritants. Interestingly, only 2 compounds - Anastrozole and 19-Norandrosterone - were predicted to be non-toxic in the *T. pyriformis* toxicity model, suggesting a limited environmental toxicity profile. These findings highlight the importance of ADMET and *in silico* toxicity screening as a preliminary step in identifying promising bioactive compounds, while simultaneously eliminating those with unfavorable pharmacokinetic or safety characteristics.

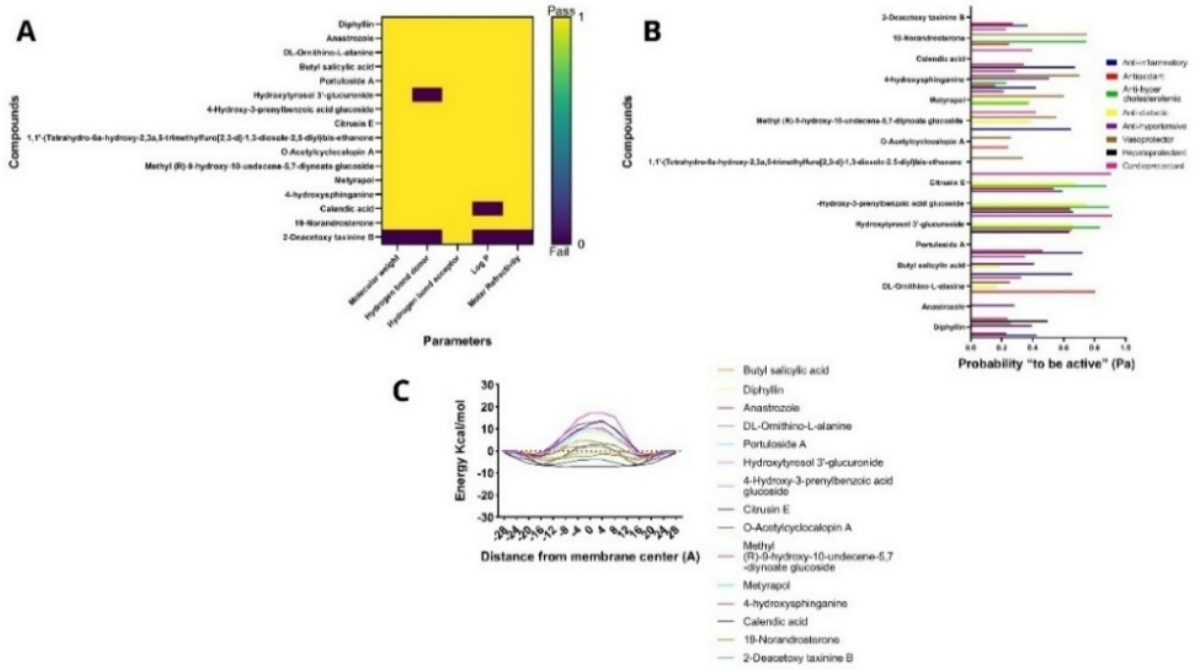

Figure 2 Pharmacokinetic profile of *Salazza zalacca* skin. (A) Lipinski's rule of 5 criteria of SZS compound. (B) Biological activity prediction of SZS compound. (C) Passive permeability membrane of SZS compound.

Biological activity and permeability of membrane

Biological activity prediction helps identify potential therapeutic roles of compounds by estimating their ability to modulate specific molecular targets or pathways relevant to diseases [13]. In parallel, membrane permeability assessment provides insight into a compound's ability to cross the cell membrane - a critical step for exerting intracellular effects and ensuring effective bioavailability [54]. In this study, biological activity predictions revealed that multiple SZS compounds may have therapeutic relevance to metabolic syndrome (MetS) (**Figure 2(B)**). Portuloside A demonstrated strong anti-inflammatory potential, DL-Ornithino-L-alanine showed antioxidant activity, Hydroxytyrosol 3'-glucuronide was predicted to be both anti-hypercholesterolemic and antidiabetic, 4-Hydroxysphinganine had antihypertensive properties, 2-Deacetoxy Taxinine B was identified as vasoprotective, while Anastrozole and 1,1'-(Tetrahydro-6a-hydroxy-2,3a,5-trimethylfuro[2,3-d]-1,3-dioxole-2,5-diyl)bis-ethanone were associated with hepatoprotective and cardioprotective activity, respectively. These findings suggest that SZS contains bioactive compounds capable of targeting multiple aspects of MetS, supporting its potential for nutraceutical or pharmaceutical development

Membrane permeability analysis further refined compound selection by evaluating their ability to penetrate cell membranes, a necessary trait for reaching intracellular targets. Compounds Butyl salicylic acid, Calendic acid, 19-Norandrosterone, and 2-Deacetoxy taxinine B were found to have low translocation energy, indicating high permeability and better cellular uptake potential (see **Figure 2(C)**). This enhances their drug-likeness and supports their prioritization in future pharmacological studies. These combined analyses provide a rational basis for selecting promising bioactive compounds for further validation.

Network construction of MetS

Network construction is a critical approach for understanding the molecular mechanisms of complex diseases like Metabolic Syndrome (MetS), by mapping interactions between genes and proteins involved in disease progression [55]. In this study, MetS-related genes were retrieved from DisGeNET, GeneCards, and NCBI databases, resulting in 226, 388, and 349 genes respectively, based on relevance scoring criteria (see Supplementary **Figures 2(A)** to **2(C)**). A Venn diagram

comparison identified 29 overlapping genes common to all 3 databases (Supplementary **Figure 2(D)**), which were used to construct a gene interaction network via the STRING database and visualized with Cytoscape.

Betweenness centrality analysis was performed to identify key regulatory genes within the network. Genes such as INS, IL-6, MTHFR, PIK3CA, PPARG, and TNF-α exhibited high betweenness centrality, indicating they serve as major hubs and potential therapeutic targets in MetS pathophysiology (Supplementary **Figure 2(E)**). Among these, TNF-α and PPARG were prioritized for further molecular docking studies due to their central roles in inflammation, insulin resistance, and lipid metabolism - core features of MetS [56]. This network analysis not only reinforces the mechanistic plausibility of SZS targeting multiple pathways but also provides rational targets for further experimental validation, underscoring the multi-target therapeutic potential of natural products in complex metabolic disorders.

Molecular docking with TNF-α

In this study, molecular docking and molecular dynamics simulations were employed to investigate the interaction of selected bioactive compounds from SZS with 2 critical protein targets - tumor necrosis factor-alpha (TNF-α) and peroxisome proliferator-activated receptor gamma (PPARG) - identified through protein-protein interaction (PPI) network analysis. These computational approaches are essential components of modern drug discovery, providing detailed insights into the binding affinity, interaction stability, and conformational behavior of ligand-protein complexes under dynamic biological conditions [15].

Molecular docking was used to predict how well SZS compounds could fit into the binding sites of TNF-α and PPARG, which are both pivotal in the pathogenesis of MetS. Docking helps identify potential lead compounds by estimating their binding energies and visualizing their interactions with key amino acid residues [13,21]. However, static docking snapshots may not fully capture the dynamic nature of protein-ligand interactions. Therefore, molecular dynamics simulations were conducted to assess the temporal stability, flexibility, and conformational changes of the docked complexes in a simulated biological environment. This step is critical for evaluating whether a compound can maintain stable binding under physiological conditions, which directly impacts its potential efficacy and safety as a therapeutic agent.

The selection of TNF-α as a molecular target is particularly relevant in the context of MetS. TNF-α is a pro-inflammatory cytokine that plays a central role in systemic inflammation and has been strongly implicated in the development of insulin resistance, a key component of MetS. Elevated TNF-α levels are frequently observed in individuals with obesity, type 2 diabetes, and cardiovascular disorders [57]. Mechanistically, TNF-α disrupts insulin signaling pathways by inducing serine phosphorylation of insulin receptor substrates and promoting the expression of other inflammatory mediators such as IL-6 and MCP-1. This cascade contributes to chronic low-grade inflammation, endothelial dysfunction, and lipid metabolism abnormalities - all hallmark features of MetS [58-60]. Therefore, inhibiting TNF-α activity has the potential to modulate the inflammatory axis of MetS and improve metabolic outcomes.

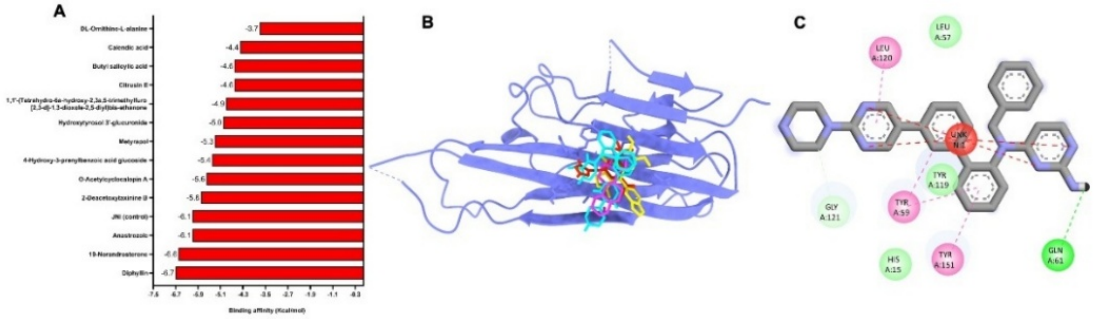

Figure 3 Molecular docking result of SZS against TNF-α. (A) Free energy binding affinity result, (B) Visualization of SZS and control binding site on TNF-α protein, (C) Interaction of the control amino acid residues on TNF-α.

Through docking analysis, 3 compounds - Anastrozole (–6.1 Kcal/mol), 19-norandosterone (–6.6 Kcal/mol), and diphyllin (–6.7 Kcal/mol) - demonstrated strong binding affinities to TNF-α, with Diphyllin showing the most favorable interactions, as shown in **Figure 3(A)**. The similarity of the binding poses of the SZS compound and the control is shown in **Figure 3(B)**. Meanwhile, the control binds to TNF-α through hydrogen bonds at GLN61 and hydrophobic interactions at UNK1, TYR59, TYR119, TYPR151, LEU120, LEU57, GLY121, and HIS15 (**Figure 3(C)**). Similarly, the SZS compounds - Diphyllin, 19-Norandosterone, and Anastrozole - exhibit comparable binding poses (**Figure 4**). Diphyllin forms hydrophobic bonds with LEU57 and TYR59, and hydrogen bonds with SER60, TYR119, LEU120, GLY121, GLY122, ILE155, and TYR151 (**Figure 4(A)**). 19-Norandosterone engages in hydrophobic bonding with TYR59 and TYR119, and hydrogen bonding with LEU57, LEU120, GLY121, and TYR151 (**Figure 4(B)**). Anastrozole interacts hydrophobically with LEU57, TYR59, and TYR119, and forms hydrogen bonds with HIS15, ILE58, SER60, GLN61, GLY121, GLY122, TYR151, and ILE155 (see **Figure 4(C)**). Similarities in the interactions between the amino acid residues of the control and the 3 compounds on the protein, including TYR59, LEU120, and TYR151, predicted that all 3 compounds mimic the control ligand's binding mode, potentially enabling them to effectively inhibit TNF-α activity. The redocking was performed on TNF-α, showing good and similar configuration with an RMSD value of 0.67 Å, as depicted in Supplementary **Figure 3(A)**.

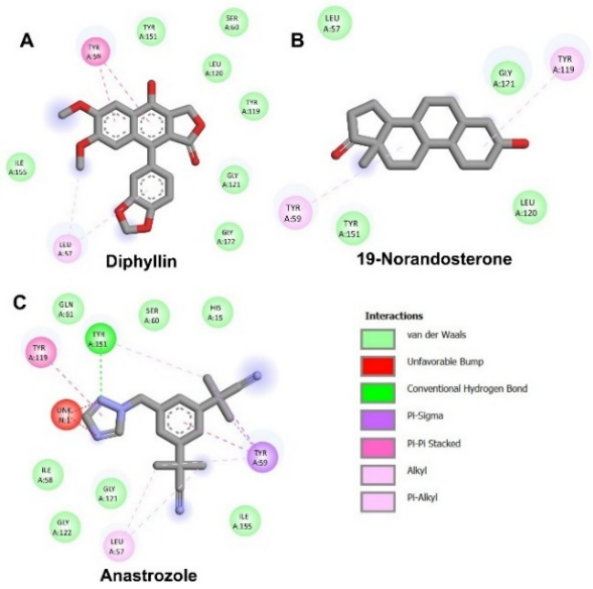

Figure 4 2D interaction of SZS compounds against TNF-α. (A) Amino acid residues of Diphyillin, (B) Amino acid residues of 19-Norandosterone, (C) Amino acid residues of Anastrozole.

Molecular dynamics (MD) simulations revealed that Diphyllin demonstrated the highest structural stability when bound to TNF-α, with a low and consistent RMSD value of 0.2 nm throughout the simulation (**Figure 5(A)**). In contrast, 19-Norandrosterone and Anastrozole exhibited significant RMSD fluctuations (up to 3 nm and 2.2 nm, respectively), indicating less stable interactions. The control ligand JNI showed moderate stability with an RMSD of 1.4 nm during the 1st 100 ns. The RMSF analysis identified Ser9 as a flexible region across all compounds, with the highest residue fluctuations observed at Glu104 (JNI), Ala22 (Norandrosterone), and Ser86 (Diphyllin), as shown in **Figure 5(B)**. Despite local flexibility, the Radius of Gyration (RoG) analysis confirmed that TNF-α maintained a stable and compact global structure (RoG range: 1.6 - 1.65 nm), as shown in **Figure 5(C)**.

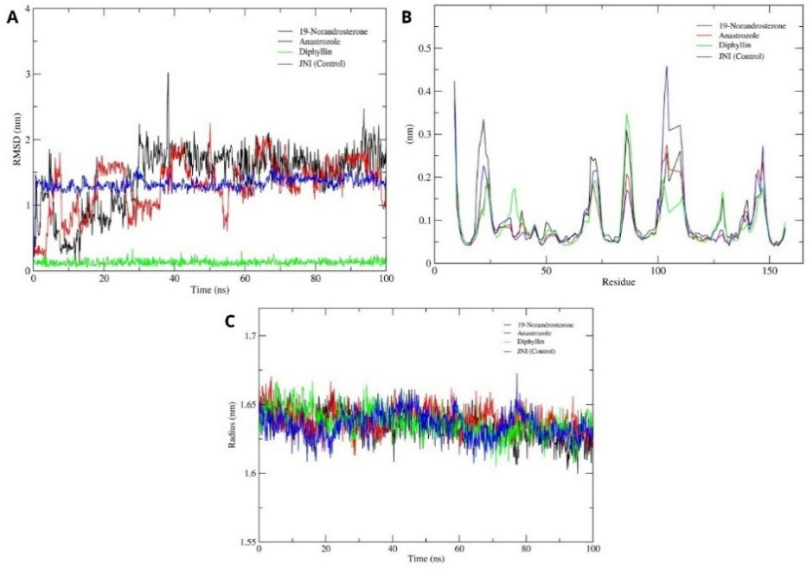

Figure 5 Molecular dynamics analysis of TNF-α. (A) RMSD analysis of SZS and control on TNF-α, (B) RMSF analysis of SZS and control on TNF-α, (C) RoG analysis of TNF-α.

Hydrogen bond occupancy supported these findings: Diphyllin formed the most stable interactions, especially with Tyr151 (1.10%), indicating strong and sustained binding. JNI and Anastrozole also showed notable hydrogen bonding, but less so than Diphyllin (see **Table 2**).

Table 2 Hydrogen bonds and occupancy between the SZS compounds and TNF-α

Compound	Donor	Acceptor	Occupancy
19-Norandrosterone	Tyr151-Side	19-Norandrosterone -Main	0.60%
	Tyr159-Side	19-Norandrosterone -Side	0.20%
Anastrozole	Anastrozole -Side	Leu37-Main	0.90 %
	Leu37-Main	Anastrozole-Side	0.50%
	His15-Side	Anastrozole-Side	0.40%
Diphyllin	Tyr151-Side	Diphyllin -Side	1.10%
JNI (Control)	JNI (Control)-Side	Gly148-Main	1.00%
	JNI (Control) -Side	Gln149-Side	0.40%

Abbreviations: TNF-α. Tumor Necrosis Factor- α; RMSD. Root-mean-square deviation; ns. Nanosecond

Free energy analysis using the MM-GBSA method ranked compound stability based on ΔTOTAL values, including; Diphyllin: –22.65 kcal/mol (strongest binding); Anastrozole: –17.72 kcal/mol; 19-Norandrosterone: –13.31 kcal/mol; and JNI (control): –25.75 kcal/mol, though weakened by high polar solvation energy (+202.58 kcal/mol), suggesting instability under physiological conditions [26] (**Table 3**).

Table 3 Free energy calculations between the active compounds and the amino acid residues of the TNF-α protein.

Compound	ΔVDWAALS (kcal/mol)	ΔEEL (kcal/mol)	ΔEGB (kcal/mol)	ΔESURF (kcal/mol)	ΔGGAS (kcal/mol)	ΔGSOLV (kcal/mol)	ΔTOTAL (kcal/mol)
19-Norandrosterone	–17.02 ± 0.48	–1.86 ± 0.01	7.77 ± 0.34	–2.20 ± 0.02	–18.88 ± 0.48	5.57 ± 0.34	–13.31 ± 0.58
Anastrozole	–20.76 ± 1.22	–1.29 ± 0.00	6.96 ± 0.32	–2.63 ± 0.03	22.04 ± 1.22	4.32 ± 0.32	–17.72 ± 1.26
Diphyllin	–27.98 ± 0.80	–3.41 ± 0.30	11.83 ± 0.45	–3.09 ± 0.03	–31.39 ± 0.85	–8.74 ± 0.46	–22.65 ± 0.97
JNI (Control)	–32.06 ± 1.20	–192.74 ± 1.84	202.58 ± 3.59	–3.53 ± 0.06	-224.81 ± 2.20	199.05 ± 3.59	–25.75 ± 4.21

Abbreviations: MM-GBSA. Molecular Mechanics - Generalized Born Surface Area; VDWAALS. Van der waals; ΔEEL. Electrostatic interactions; ΔEGB. Solvation energy; ΔESURF. Fluctuations energy; ΔGGAS. Gibbs free energy of solvation; ΔGSOLV. Insolvation-free energy.

These findings showed Diphyllin demonstrated the most favorable interaction with TNF-α across all analyses - exhibiting high binding stability, strong hydrogen bonding, and favorable energy profiles - positioning it as the most promising candidate among the tested SZS compounds. Diphyllin could act as a potential TNF-α inhibitor, contributing to the suppression of inflammation and amelioration of insulin resistance in MetS. The integration of molecular docking and molecular dynamics in this study provided a robust framework for evaluating the pharmacological potential of SZS-derived compounds. By targeting TNF-α - an inflammatory mediator intricately linked to MetS pathology - this approach not only identifies promising therapeutic candidates but also strengthens our mechanistic understanding of how these compounds may exert their beneficial effects in the context of metabolic disease.

Molecular docking with PPARG

The comprehensive computational analysis of SZS-derived compounds interacting with peroxisome proliferator-activated receptor gamma (PPARG) highlights their potential in modulating key metabolic pathways relevant to MetS, as shown in **Figure 6**. Among the 16 active compounds screened, 6 - hydroxytyrosol-3-glucuronide, citrusin-E, 19-norandosterone, 4-hydroxy-3-prenylbenzoic acid glucoside, diphyllin, and anastrozole - demonstrated stronger binding affinities to PPARG than the standard control ligand BRL, as determined by molecular docking (see **Figure 6(A)**). The similarity of the binding poses of the SZS compound and the control is shown in **Figure 6(B)**. Meanwhile, the control binds to PPARG through hydrogen bonds at SER342; and hydrophobic interaction at UNK1, ALA292, ILE326, SER289, ARG288, TYR327, MET364, LEU330, GLU343, CYS285, VAL339, LEU228, LEU333, PHE363, and LEU340 (**Figure 6(C)**). Notably, anastrozole exhibited the highest binding affinity (–7.9 kcal/mol), followed closely by diphyllin (–7.4 kcal/mol) and 4-hydroxy-3-prenylbenzoic acid glucoside (–7.3 kcal/mol).

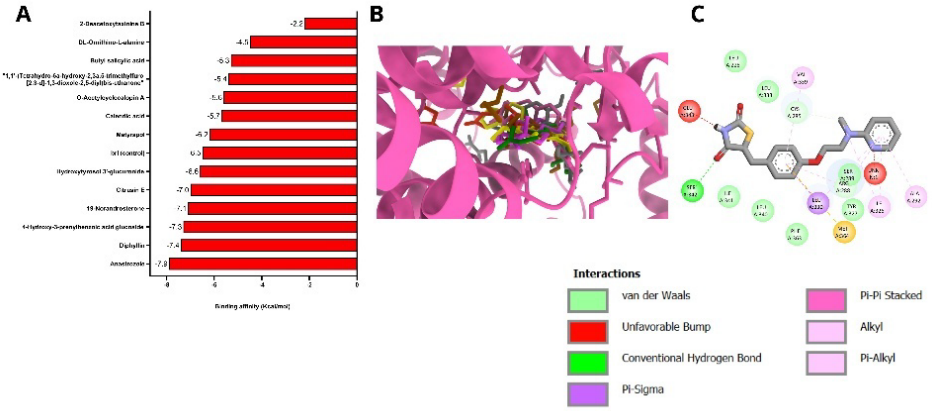

Figure 6 Molecular docking result of SZS against PPARG. (A) Free energy binding affinity result, (B) Visualization of SZS and control binding sites on PPARG protein, (C) Interaction of the control amino acid residues on PPARG.

These results also showed that SZS compounds can occupy the same ligand-binding pocket as BRL (**Figures 7(A)** to **7(F)**), interacting with critical amino acid residues such as CYS285, ARG288, SER289, and LEU330, which are essential for PPARG activation and regulation. The results of the redocking to PPARG indicate a good and similar configuration, with an RMSD value of 1.16 Å, as shown in Supplementary **Figure 3(B)**.

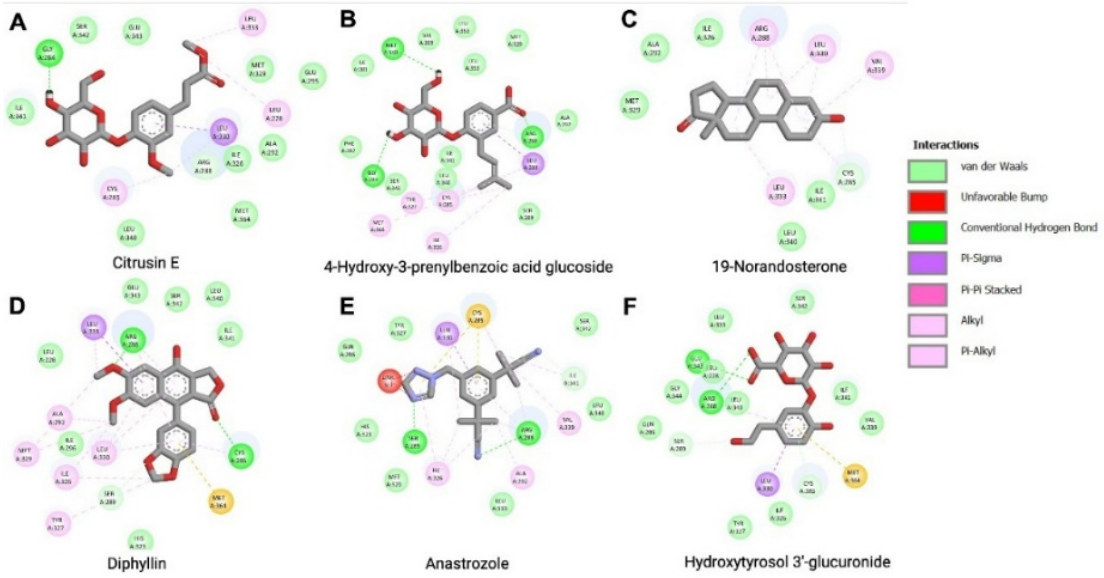

Figure 7 2D interaction of SZS compounds against PPARG. (A) Amino acid residues of Citrusin E, (B) Amino acid residues of 4-Hydroxy-3-prenylbenzoic acid glucoside, (C) Amino acid residues of 19-Norandosterone, (D) Amino acid residues of Diphyllin, (E) Amino acid residues of Anastrozole, (F) Amino acid residues of Hydroxytyrosol 3'-glucuronide

Molecular dynamics simulations over 100 nanoseconds further evaluated the stability and conformational dynamics of the ligand-PPARG complexes, as shown in **Figure 8(A)**. The compounds such as Citrusin-E and 4-hydroxy-3-prenylbenzoic acid glucoside showed consistently low RMSD values around 0.25 nm throughout the simulation, indicating high structural stability. Diphyllin and 19-norandosterone also maintained relatively stable conformations, with moderate fluctuations ranging from 0.1 to 0.5 nm. In contrast, BRL (control) exhibited significant instability, with sharp RMSD deviations

from 0.5 to 2.5 nm at around 50 ns. RMSF analysis revealed local flexibility in certain protein residues [61], with 19-norandosterone causing the highest fluctuation at Glu207 (0.8110 nm), while Citrusin-E and diphyllin induced moderate flexibility at Ser428 and other binding site residues (**Figure 8(B)**). The radius of gyration (RoG) values of the complexes ranged between 1.85 and 1.96 nm (**Figure 8(C)**), indicating that PPARG possesses a relatively flexible tertiary structure compared to TNF-α, potentially allowing better ligand accommodation and conformational adaptation.

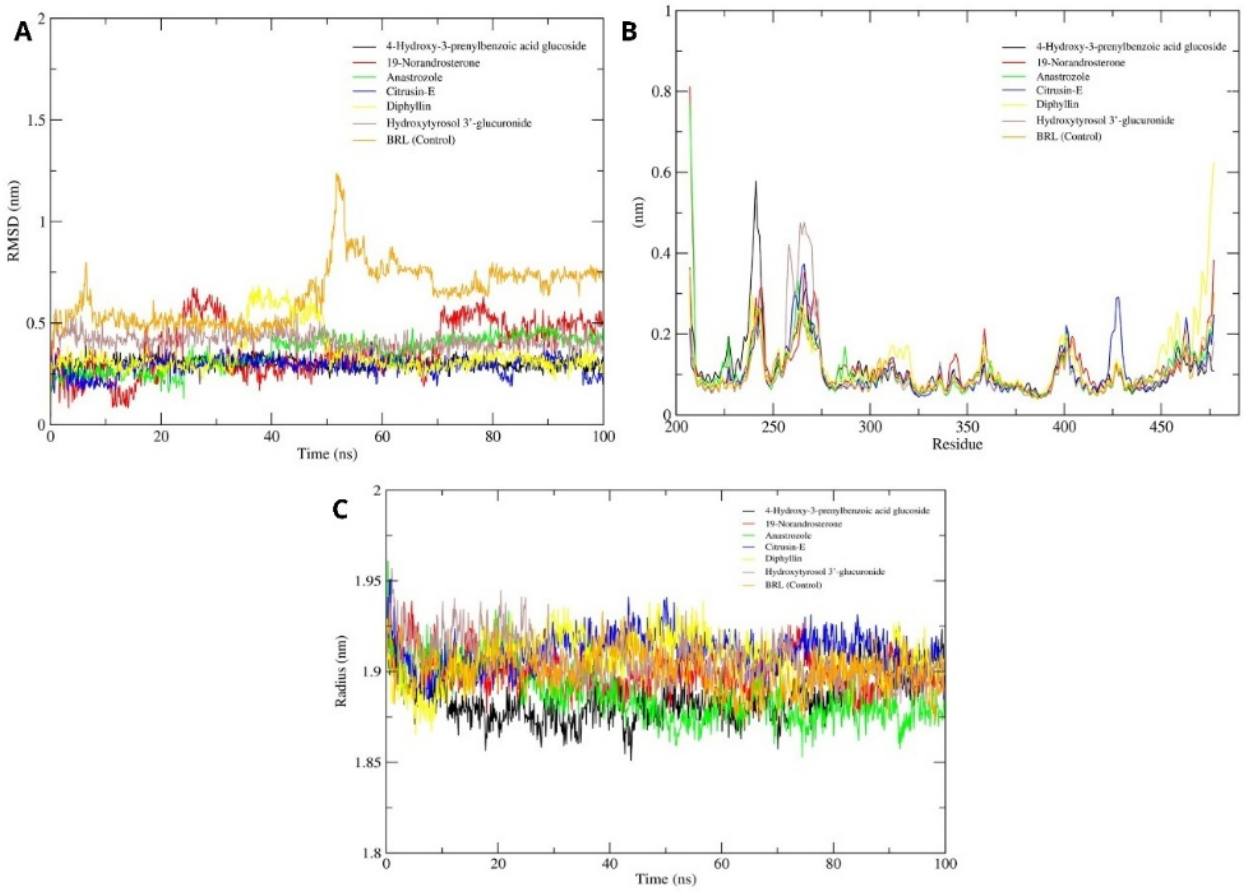

Figure 8 Molecular dynamics analysis of PPARG. (A) RMSD analysis of SZS and control on PPARG, (B) RMSF analysis of SZS and control on PPARG, (C) RoG analysis of PPARG

Abbreviations: PPARG. Peroxisome Proliferator-Activated Receptor Gamma; RMSD. Root-mean-square deviation; ns. Nanosecond.

Hydrogen bond occupancy analysis provided further insights into the stability and strength of interactions, illustrated in **Table 4**. Hydroxytyrosol-3-glucuronide displayed the highest hydrogen bond occupancy, particularly with Ser342 (10.48%), followed by Diphyllin (5.89%) and Anastrozole (4.19%). These interactions indicate a strong and persistent hydrogen bonding network, contributing to the overall stability of these ligand-protein complexes. Interestingly, while Hydroxytyrosol-3-glucuronide had the highest hydrogen bond occupancy, it showed the least favorable total binding energy in MM-GBSA calculations, with a ΔTOTAL of –27.57 kcal/mol. In contrast, Citrusin-E and Diphyllin demonstrated the most favorable binding free energies (–39.20 and –38.18 kcal/mol, respectively), driven by strong van der Waals forces and moderate electrostatic contributions, despite their high polar solvation energies (see **Table 5**). This suggests that these 2 compounds form highly stable complexes with PPARG in aqueous environments.

Table 4 Hydrogen bonds and occupancy between the SZS compounds and PPARG.

Compound	Donor	Acceptor	Occupancy
4-Hydroxy-3-prenylbenzoic acid glucoside	4-Hydroxy-3-prenylbenzoic acid glucoside -Side	Met348-Side	0.30%
	4-Hydroxy-3-prenylbenzoic acid glucoside -Side	Leu340-Main	0.20%
19-Norandrosterone	Arg288-Side	19-Norandrosterone -Main	0.50%
	19-Norandrosterone -Side	Cys285-Main	0.40%
	Leu228-Main	19-Norandrosterone -Main	2.79%
Anastrozole	Arg288-Main	Anastrozole -Side	4.19%
	Anastrozole -Side	Cys285-Main	0.20%
Citrusin-E	Ser342-Side	Citrusin-E -Side	0.20%
	Citrusin-E -Side	Gly284-Main	0.30%
	Ser342-Main	Citrusin-E-Side	0.20%
Diphyllin	Ser342-Main	Diphyllin -Side	5.89%
Hydroxytyrosol 3'-glucuronide	Ser342-Main	Hydroxytyrosol 3'-glucuronide -Side	10.48%
	Hydroxytyrosol 3'-glucuronide -Side	Ser289-Side	1.70%
	Hydroxytyrosol 3'-glucuronide -Side	Cys285-Main	0.30%
	Ser289-Side	Hydroxytyrosol 3'-glucuronide -Side	0.50%
	Lys261-Side	Hydroxytyrosol 3'-glucuronide -Side	0.30%
BRL (control)	BRL (control)-Side	Glu343-Side	0.50%
	BRL (control)-Side	Ser342-Side	0.30%
	BRL (control)-Side	Arg288-Main	0.70%

Collectively, these findings underscore the potential of several SZS compounds - particularly diphyllin and Citrusin-E - as promising PPARG modulators for the treatment of metabolic syndrome. Their strong binding affinities, stable dynamic behavior, and favorable interaction energies suggest that they could enhance insulin sensitivity and modulate lipid metabolism by targeting PPARG.

Table 5 Free energy calculations between the active compounds and the amino acid residues of the PPARG protein.

Compound	ΔVDWAALS (kcal/mol)	ΔEEL (kcal/mol)	ΔEGB (kcal/mol)	ΔESURF (kcal/mol)	ΔGGAS (kcal/mol)	ΔGSOLV (kcal/mol)	ΔTOTAL (kcal/mol)
4-Hydroxy-3-prenylbenzoic acid glucoside	–45.87 ± 0.83	–1.70 ± 2.16	17.50 ± 0.71	–6.73 ± 0.02	–47.57 ± 2.32	10.77 ± 0.71	–36.80 ± 2.42
19-Norandrosterone	–39.57 ± 0.64	–3.92 ± 1.62	12.19 ± 1.60	–4.79 ± 0.06	–43.50 ± 1.75	7.40 ± 1.60	–36.10 ± 2.37
Anastrozole	–46.35 ± 0.19	–5.60 ± 0.68	14.27 ± 0.21	–5.86 ± 0.06	–51.95 ± 0.71	8.41 ± 0.22	–43.54 ± 0.74
Citrusin-E	–48.26 ± 0.82	–9.43 ± 2.38	25.63 ± 1.10	–7.14 ± 0.03	–57.69 ± 2.52	18.49 ± 1.10	–39.20 ± 2.75
Diphyllin	–48.62 ± 0.96	–7.50 ± 0.25	24.04 ± 0.52	–6.10 ± 0.03	–56.12 ± 0.99	17.93 ± 0.52	–38.18 ± 1.11
Hydroxytyrosol 3'-glucuronide	–38.98 ± 0.68	–6.04 ± 1.78	23.33 ± 0.93	–5.88 ± 0.03	–45.02 ± 1.91	17.46 ± 0.93	–27.57 ± 2.12
BRL (control)	–49.52 ± 0.14	–0.92 ± 0.41	13.82 ± 0.19	–5.70 ± 0.02	–50.43 ± 0.43	8.11 ± 0.19	–42.32 ± 0.47

Abbreviations: MM-GBSA. Molecular Mechanics - Generalized Born Surface Area; VDWAALS. Van der waals; ΔEEL. Electrostatic interactions; ΔEGB. Solvation energy; ΔESURF. Fluctuations energy; ΔGGAS. Gibbs free energy of solvation; ΔGSOLV. Insolvation-free energy

Antioxidant and enzyme inhibition activity

The antioxidant potential of the SZS ethanol extract was assessed using 2 widely recognized free radical scavenging assays - ABTS and DPPH - which serve as proxies for evaluating the extract's capacity to neutralize ROS, as shown in **Figure 9**. These ROS, such as free radicals, are known to contribute significantly to oxidative stress, a pathological state associated with the onset and progression of chronic conditions, including MetS [62]. Given that oxidative stress plays a pivotal role in insulin resistance, inflammation, and endothelial dysfunction - all hallmark features of MetS [1,63] - identifying plant-based antioxidants with therapeutic relevance is a critical step in natural product drug discovery and functional food development.

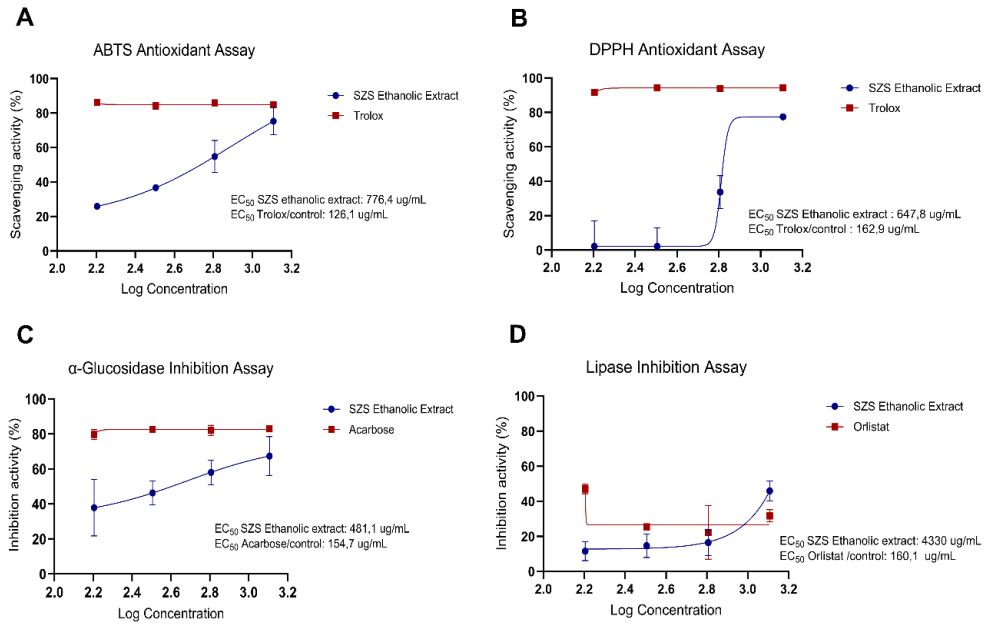

Figure 9 The result of biochemical assay. (A) ABTS Antioxidant Assay, (B) DPPH Antioxidant Assay, (C) α-Glucosidase Inhibition Assay, (D) Lipase Inhibition Assay.

Abbreviations: ABTS. 2,2'-Azino-bis(3-ethylbenzothiazoline-6-sulfonic acid; DPPH. 2,2-Diphenyl-1-picrylhydrazyl; EC50. Half maximal effective concentration.

In the ABTS assay, the SZS ethanol extract demonstrated dose-dependent scavenging activity; however, its effectiveness was inferior to the synthetic antioxidant Trolox (**Figure 9(A)**), as indicated by its higher EC_{50} value (776.4 µg/mL vs. 126.1 µg/mL for Trolox). Similarly, in the DPPH assay, the extract exhibited moderate free radical scavenging capacity with an EC_{50} value of 647.8 µg/mL, compared to 162.9 µg/mL for Trolox (see **Figure 9(B)**). These results indicate that while the SZS extract possesses antioxidant properties, its potency is relatively moderate when benchmarked against potent standard antioxidants.

When compared with other studies, such as the SPE Sumalee cultivar which demonstrated much stronger DPPH (IC_{50} = 8.87 µg/mL) and ABTS (IC_{50} = 22.48 µg/mL) activity, the current SZS ethanol extract appears less efficient [11]. Similarly, Salacca *sedulis* skin, another closely related variety, exhibited potent antioxidant effects with DPPH and ABTS IC_{50} values of 2.93 and 7.93 µg/mL, respectively [11]. These comparative findings suggest that the antioxidant capacity of SZS may be cultivar-dependent, and the phenolic, terpenoid, and glycoside content in different varieties may significantly influence bioactivity. Moreover, a study on the Bali cultivar of salak skin showed up to 73.13% DPPH inhibition [64], further underscoring the variability in antioxidant potency among salak variants. The relatively moderate antioxidant capacity of the current SZS ethanol extract, while not as potent as some other cultivars, remains biologically relevant. This is particularly important in the context of MetS, where chronic oxidative stress is implicated in lipid peroxidation, mitochondrial dysfunction, and inflammatory signaling. Natural antioxidants such as those in SZS extracts could provide synergistic benefits when used alongside other therapies aimed at mitigating insulin resistance and inflammation. The phenolic compounds, terpenoids, and glycosides detected in the extract are known to modulate oxidative pathways, and even modest free radical scavenging could contribute to redox balance over time, especially in dietary or supplementary applications [65,66]. Antioxidants derived from natural sources are increasingly favored due to their lower toxicity and ability to target multiple molecular pathways. The current findings support the potential utility of SZS as a complementary therapeutic agent for reducing oxidative stress in MetS, warranting further phytochemical profiling and *in vivo* studies to fully explore its clinical relevance.

Carbohydrate and lipid metabolism are crucial for maintaining overall metabolic health and preventing metabolic syndrome, which includes conditions such as obesity, high blood pressure, elevated blood sugar, and abnormal lipid levels [67]. Individuals with metabolic syndrome often experience impaired carbohydrate and lipid metabolism, leading to insulin resistance, hyperglycemia, and dyslipidemia [68]. These metabolic abnormalities contribute to the development and progression of metabolic syndrome, which is strongly associated with an increased risk of cardiovascular disease and type 2 diabetes [69]. To evaluate the effect of SZS ethanol extract on carbohydrate and lipid metabolism, α-glucosidase and lipase inhibition assays were performed. These assays are commonly used to measure the activity of these enzymes and provide valuable information about their inhibition, that plays a significant role in carbohydrate and lipid metabolism

The result shows that increasing the concentration of SZS ethanol extract increases the α-glucosidase inhibitory activity. The EC50 values of SZS ethanol extract and acarbose were 481.1 and 154.7 µg/mL, respectively, as shown in **Figure 9(C)**. Several studies have reported the antidiabetic effects of SZS from various cultivars. In an *in vitro* study, the highest anti-diabetic activity through glucosidase enzyme inhibition was found in the Salak Manonjaya cultivar (IC50: 17.9 µl/dl) [66]. *In vivo*, SZS from the Balikpapan cultivar was reported to reduce blood glucose levels in diabetic model rats, showing 40.94% inhibition at a dose of 210 mg/kgBW [70]. In addition, SZS from Medan cultivar exhibited anti-hyperglycemic effects at the lowest dose (60 mg/200 gBW) in alloxan-induced Wistar rats [12].

The lipase inhibition assay shows that SZS ethanol extract can inhibit lipase enzyme activity, though less effectively than the positive control, orlistat, with EC50 values of 4,330 and 160.1 µg/mL, respectively, as shown in **Figure 9(D)**. While the inhibitory effect of SZS is not as potent as the control, these findings highlight that the ethanol extract of SZS does possess inhibitory activity against both lipase and α-glucosidase. The lipase inhibition assay in this study is the 1st to

assess the anti-lipidemic effect of SZS, and no prior studies have documented this activity. Lipase is an enzyme responsible for breaking down triglycerides into fatty acids and glycerol, which are then absorbed by the body. By inhibiting lipase activity, SZS may help reduce fat absorption during digestion, potentially leading to reduced caloric intake and weight loss. This suggests that SZS could be beneficial in reducing fat absorption and, by extension, may help mitigate the risk of obesity. The inhibition of lipase activity could also have implications for the management of conditions such as obesity and hyperlipidemia [71,72].

Limitation of study

We acknowledge several limitations in our study regarding the efficacy of SZS as an Indonesian herbal medicine for metabolic syndrome (MetS). Our research is primarily based on predictive computational modeling and biochemical assays evaluating enzymatic activity. This study lacks *in vivo* validation and does not assess pharmacokinetics in biological systems. Although molecular docking results suggest potential binding of key SZS compounds to targets such as TNF-α and PPARG, these interactions remain hypothetical until verified by structural biology techniques such as X-ray crystallography or cryo-electron microscopy (cryo-EM). The safety profile of the ethanol extract of SZS has not yet been established; comprehensive toxicity assessments are essential to ensure its suitability for therapeutic use. Nevertheless, SZS demonstrates significant potential as an Indonesian herbal medicine for managing MetS due to its multi-target mechanisms, including anti-inflammatory and insulin-sensitizing effects. The predicted interactions with central MetS-related targets such as TNF-α and PPARG suggest that SZS may modulate key metabolic and inflammatory pathways. Further pharmacological studies and clinical trials will be critical to confirm its efficacy, optimize dosage, and evaluate its long-term safety. These future efforts will help bridge the gap between traditional herbal use and evidence-based therapeutic application in the management of MetS

Conclusions

In conclusion, the ethanol extract of SZS exhibits significant antioxidant, antihyperglycemic, and antihyperlipidemic activities through *in vitro* assay. Furthermore, diphyllin, anastrozole, and 19-norandosterone demonstrated promising interaction with TNF-α and PPARG, suggesting SZS extract may support metabolic syndrome therapy by modulating inflammation and metabolic pathways. SZS can be a good consideration as an adjuvant or nutraceutical through further studies to support safety, optimal dosage, and minimizing adverse side effects. SZS also has the potential as an adjuvant agent that is expected to synergize with existing MetS drugs to ensure better control of the disease.

Acknowledgements

The authors would like to express their gratitude to the staff and laboratory assistants of the Pharmacology Laboratory, Faculty of Medicine, Universitas Brawijaya, Indonesia, for their technical assistance. Special recognitions are also given to the Faculty of Medicine of Universitas Brawijaya for their funding support with Funding Number: 3173.2/1/UN10.F08/PN/2023.

Declaration of Generative AI in Scientific Writing

The authors acknowledge the use of generative artificial intelligence tools (deepL.com) in the preparation of this manuscript, particularly for editing and grammar correction. No content generation or data interpretation was conducted by artificial intelligence. The authors are completely responsible for the content and conclusions of this work.

CRediT Author Statement

Diana Yuswanti Putri: Conceptualization, Data curation, Formal analysis, Funding acquisition, Investigation, Software, Supervision, Validation, Visualization, Writing – original draft, Writing – review and editing

Yuyun Yueniwati: Conceptualization, Data curation, Formal analysis, Funding acquisition, Investigation, Software, Supervision, Validation, Visualization, Writing – original draft, Writing – review and editing

Sri Utami: Methodology, Project administration, Resources, Writing – original draft, Writing - review & editing

Mokhamad Fahmi Rizki Syaban: Data curation, Formal analysis, Investigation, Resources, Writing – original draft, Writing – review & editing, Visualization

Nirmala Halid: Validation, Visualization, Writing – original draft, Writing – review and editing

Purnawan Pontana Putra: Data curation, Methodology, validation, writing – review & editing

Sastia Prama Putri: Software, Supervision, Validation.

Husnul Khotimah: Methodology, Writing – review & editing, Visualization.

References

[1] HH Wang, DK Lee, M Liu, P Portincasa and DQH Wang. Novel insights into the pathogenesis and management of the metabolic syndrome. *Pediatric Gastroenterology, Hepatology & Nutrition* 2020; **23(3)**, 189-230.

[2] EH Herningtyas and TS Ng. Prevalence and distribution of metabolic syndrome and its components among provinces and ethnic groups in Indonesia. *BMC Public Health* 2019; **19(1)**, 377.

[3] G Hirode and RJ Wong. Trends in the prevalence of metabolic syndrome in the United States, 2011-2016. *JAMA* 2020; **323(24)**, 2526-2528.

[4] S Uddin, PR Brooks and TD Tran. Chemical characterization, α-glucosidase, α-amylase and lipase inhibitory properties of the Australian honey bee propolis. *Foods* 2022; **11(13)**, 1964.

[5] M Hawash, N Jaradat, S Shekfeh, M Abualhasan, AM Eid and L Issa. Molecular docking, chemo-informatic properties, alpha-amylase, and lipase inhibition studies of benzodioxol derivatives. *BMC Chemistry* 2021; **15**, 40.

[6] JK Sethi and GS Hotamisligil. Metabolic messengers: Tumour necrosis factor. *Nature Metabolism* 2021; **3(10)**, 1302-1312.

[7] M Botta, M Audano, A Sahebkar, CR Sirtori, N Mitro and M Ruscica. PPAR agonists and metabolic syndrome: An established role? *nternational Journal of Molecular Sciences* 2018; **19(4)**, 1197.

[8] Q Haguet, FL Joubioux, V Chavanelle, H Groult, N Schoonjans, C Langhi, A Michaux, YF Otero, N Boisseau, SL Peltier, P Sirvent and T Maugard. Inhibitory potential of α-amylase, α-glucosidase, and pancreatic lipase by a formulation of five plant extracts: TOTUM-63. *International Journal of Molecular Sciences* 2023; **24(4)**, 3652.

[9] MM Algandaby. Crocin prevents metabolic syndrome in rats via enhancing PPAR-gamma and AMPK. *Saudi Journal of Biological Sciences* 2020; **27(5)**, 1310-1316.

[10] E Girsang, INE Lister, CN Ginting, A Khu, B Samin, W Widowati, S Wibowo and R Rizal. Chemical constituents of snake fruit (*Salacca zalacca* (gaert.) voss) peel and *in silico* anti-aging analysis. *Molecular and Cellular Biomedical Sciences* 2019; **3(2)**, 122-128.

[11] M Kanlayavattanakul, N Lourith, D Ospondpant, U Ruktanonchai, S Pongpunyayuen and C Chansriniyom. Salak plum peel extract as a safe and efficient antioxidant appraisal for cosmetics. *Bioscience, Biotechnology, and Biochemistry* 2013; **77(5)**, 1068-1074.

[12] M Marzuki, E Girsang, AN Nasution and INE Lister. Anti-diabetic effect of snake fruit skin extract in alloxan-induced Wistar rat. *International Journal of Health and Pharmaceutical* 2022; **3(1)**, 146-153.

[13] S Utami, MFR Syaban, DY Putri, VAG Hose, H Khotimah and Y Yueniwati. Bioinformatics examination of quercetin from *Salacca zalacca* skin, fruit, and seed as a potent active compounds against hypercholesterolemia via PCSK9 inhibition. *Trends in Science* 2025; **22(4)**, 9237.

[14] A Daina, O Michielin and V Zoete. SwissADME: A free web tool to evaluate pharmacokinetics, drug-likeness and medicinal chemistry friendliness of small molecules. *Scientific Reports* 2017; **7(1)**, 42717.

[15] MFR Syaban, RF Muhammad, B Adnani, GFA Putra, NE Erwan, SD Arviana, AD Krisnayana and DB Kurniawan. Molecular docking studies of interaction curcumin against beta-secretase 1, amyloid A4 Protein, gamma-secretase and glycogen synthase kinase-3β as target therapy for Alzheimer disease. *Research Journal of Pharmacy and Technology* 2022; **15(7)**, 3069-3074.

[16] DA Filimonov, AA Lagunin, TA Gloriozova, AV Rudik, DS Druzhilovskii, PV Pogodin and VV Poroikov. Prediction of the biological activity spectra of organic compounds using the pass

online web resource. *Chemistry of Heterocyclic Compounds* 2014; **50(3)**, 444-457.

[17] AL Lomize and ID Pogozheva. Physics-based method for modeling passive membrane permeability and translocation pathways of bioactive molecules. *Journal of Chemical Information and Modeling* 2019; **59(7)**, 3198-3213.

[18] EF Pettersen, TD Goddard, CC Huang, EC Meng, GS Couch, TI Croll, JH Morris and TE Ferrin. UCSF CHIMERAX: Structure visualization for researchers, educators, and developers. *Protein Science* 2021; **30(1)**, 70-82.

[19] W Luo, J Deng, J He, L Yin, R You, L Zhang, J Shen, Z Han, F Xie, J He and Y Guan. Integration of molecular docking, molecular dynamics and network pharmacology to explore the multi-target pharmacology of fenugreek against diabetes. *Journal of Cellular and Molecular Medicine* 2023; **27(14)**, 1959-1974.

[20] O Daoui, S Elkhattabi and S Chtita. Rational design of novel pyridine-based drugs candidates for lymphoma therapy. *Journal of Molecular Structure* 2022; **1270**, 133964.

[21] SD Arviana, Y Yueniwati, M Rahayu and MFR Syaban. 7,8-dihydroxyflavone as a neuroprotective agent in ischemic stroke through the regulation of HIF-1α protein. *Research Journal of Pharmacy and Technology* 2022; **15(9)**, 3980-3986.

[22] EC Meng, TD Goddard, EF Pettersen, GS Couch, ZJ Pearson, JH Morris and TE Ferrin. UCSF ChimeraX: Tools for structure building and analysis. *Protein Science* 2023; **32(11)**, e4792.

[23] Wahono CS, Syaban MFR, Pratama MZ, et al. Exploring the potential of phytoconstituents from *Phaseolus vulgaris* L against C-X-C motif chemokine receptor 4 (CXCR4): A bioinformatic and molecular dynamic simulations approach. *Egyptian Journal of Medical Human Genetics* 2024; **25(1)**, 52.

[24] DVD Spoel, E Lindahl, B Hess, G Groenhof, AE Mark and HJC Berendsen. GROMACS: Fast, flexible, and free. *Journal of Computational Chemistry* 2005; **26(16)**, 1701-1718.

[25] M Yang, Z Bo, T Xu, B Xu, D Wang and H Zheng. Uni-GBSA: An open-source and web-based automatic workflow to perform MM/GB(PB)SA calculations for virtual screening. *Briefings in Bioinformatics* 2023; **24(4)**, bbad218.

[26] MS Valdés-Tresanco, ME Valdés-Tresanco, PA Valiente and E Moreno. gmx_MMPBSA: A new tool to perform end-state free energy calculations with GROMACS. *Journal of Chemical Theory and Computation* 2021; **17(10)**, 6281-6291.

[27] T Shimamura, Y Sumikura, T Yamazaki, A Tada, T Kashiwagi, H Ishikawa, T Matsui, N Sugimoto, H Akiyama and H Ukeda. Applicability of the DPPH assay for evaluating the antioxidant capacity of food additives - inter-laboratory evaluation study. *Analytical Sciences* 2014; **30(7)**, 717-721.

[28] F Nurkolis, Hardinsyah, VM Yusuf, M Yusuf, RJ Kusuma, WB Gunawan, IW Hendra, S Radu, NA Taslim, N Mayulu, N Sabrina, A Tsopmo, R Kurniawan, CF Theodorea, E Idrus and TE Tallei. Metabolomic profiling, *in vitro* antioxidant and cytotoxicity properties of caulerpa racemosa: Functional food of the future from algae. *Europe PMC*. 2024. https://doi.org/10.21203/rs.3.rs-2158307/v2

[29] J Unuofin, G Otunola and A Afolayan. *In vitro* α-amylase, α-glucosidase, lipase inhibitory and cytotoxic activities of tuber extracts of *Kedrostis africana* (L.) Cogn. *Heliyon* 2018; **4(9)**, e00810.

[30] HK Permatasari, F Nurkolis, WB Gunawan, VM Yusuf, M Yusuf, RJ Kusuma, N Sabrina, FR Muharram, NA Taslim, N Mayulu, SC Batubara, M Samtiya, H Hardinsyah and A Tsopmo. Modulation of gut microbiota and markers of metabolic syndrome in mice on cholesterol and fat enriched diet by butterfly pea flower kombucha. *Current Research in Food Science* 2022; **5(7)**, 1251-1265.

[31] AS Marchev, LV Vasileva, KM Amirova, MS Savova, ZP Balcheva-Sivenova and MI Georgiev. Metabolomics and health: from nutritional crops and plant-based pharmaceuticals to profiling of human biofluids. *Cellular and Molecular Life Sciences* 2021; **78(19-20)**, 6487-6503.

[32] JL Wolfender, G Marti, A Thomas and S Bertrand. Current approaches and challenges for the metabolite profiling of complex natural extracts.

Journal of Chromatography A 2015; **1382**, 136-164.

[33] J Dai and RJ Mumper. Plant phenolics: Extraction, analysis and their antioxidant and anticancer properties. *Molecules* 2010; **15(10)**, 7313-7352.

[34] F Shahidi and P Ambigaipalan. Phenolics and polyphenolics in foods, beverages and spices: Antioxidant activity and health effects - a review. *Journal of Functional Foods* 2015; **18(B)**, 820-897.

[35] H Khan, M Saeedi, SM Nabavi, MS Mubarak and A Bishayee. Glycosides from medicinal plants as potential anticancer agents: Emerging trends towards future drugs. *Current Medicinal Chemistry* 2019; **25(13)**, 2389-2406.

[36] L Wu, MI Georgiev, H Cao, L Nahar, HR El-Seedi, SD Sarker, J Xiao and B Lu. Therapeutic potential of phenylethanoid glycosides: A systematic review. *Medicinal Research Reviews* 2020; **40(6)**, 2605-2649.

[37] DS Arora and H Sood. *In vitro* antimicrobial potential of extracts and phytoconstituents from *Gymnema sylvestre* R.Br. leaves and their biosafety evaluation. *AMB Express* 2017; **7(1)**, 115.

[38] F Marangoni, C Agostoni, C Borghi, AL Catapano, H Cena, A Ghiselli, CL Vecchia, G Lercker, E Manzato, A Pirillo, G Riccardi, P Risé, F Visioli and A Poli. Dietary linoleic acid and human health: Focus on cardiovascular and cardiometabolic effects. *Atherosclerosis* 2020; **292**, 90-98.

[39] E Girsang, INE Lister, CN Ginting, A Khu, B Samin, W Widowati, S Wibowo and R Rizal. Chemical constituents of snake fruit (*Salacca zalacca* (Gaert.) Voss) Peel and *in silico* anti-aging analysis. *Molecular and Cellular Biomedical Science* 2019; **3(2)**, 122.

[40] M Marzuki, E Girsang, AN Nasution and INE Lister. Anti-diabetic effect of snake fruit skin extract in alloxan-induced Wistar rat. *International Journal of Health and Pharmaceutical* 2022; **3**, 146-153.

[41] JF Xiao, B Zhou and HW Ressom. Metabolite identification and quantitation in LC-MS/MS-based metabolomics. *TrAC Trends in Analytical Chemistry* 2012; **32**, 1-14.

[42] E Gorrochategui, J Jaumot, S Lacorte and R Tauler. Data analysis strategies for targeted and untargeted LC-MS metabolomic studies: Overview and workflow. *TrAC Trends in Analytical Chemistry* 2016; **82(1)**, 425-442.

[43] Tiwari BK. Ultrasound: A clean, green extraction technology. *TrAC Trends in Analytical Chemistry* 2015; **71**, 100-109.

[44] S Sasidharan, Y Chen, D Saravanan, KM Sundram and LY Latha. Extraction, isolation and characterization of bioactive compounds from plants' extracts. *African Journal of Traditional, Complementary and Alternative Medicines* 2011; **8(1)**, 1-10.

[45] S Shen, C Zhan, C Yang, AR Fernie and J Luo. Metabolomics-centered mining of plant metabolic diversity and function: Past decade and future perspectives. *Molecular Plant* 2023; **16(1)**, 43-63.

[46] CA Lipinski, F Lombardo, BW Dominy and PJ Feeney. Experimental and computational approaches to estimate solubility and permeability in drug discovery and development settings. *Advanced Drug Delivery Reviews* 2001; **46(1-3)**, 3-26.

[47] PD Leeson and B Springthorpe. The influence of drug-like concepts on decision-making in medicinal chemistry. Nat Rev Drug Discov 2007; **6(11)**, 881-890.

[48] U Vijay, S Gupta, P Mathur, P Suravajhala and P Bhatnagar. Microbial mutagenicity assay: Ames test. *Bio-protocol* 2018; **8(6)**, e2763.

[49] C Stergiopoulos, F Tsopelas and K Valko. Prediction of hERG inhibition of drug discovery compounds using biomimetic HPLC measurements. *ADMET & DMPK* 2021; **9(3)**, 191-207.

[50] S Kalyaanamoorthy, SM Lamothe, X Hou, TC Moon, HT Kurata, M Houghton and KH Barakat. A structure-based computational workflow to predict liability and binding modes of small molecules to hERG. *Scientific Reports* 2020; **10(1)**, 16262.

[51] P Francis and VJ Navarro. *Drug-induced hepatotoxicity.* StatPearls Publishing, Treasure Island, Florida, USA, 2025.

[52] GH Ta, CF Weng and MK Leong. *In silico* prediction of skin sensitization: Quo vadis? *Frontiers in Pharmacology* 2021; **12**, 655771.

[53] F Cheng, J Shen, Y Yu, W Li, G Liu, PW Lee and Y Tang. *In silico* prediction of Tetrahymena pyriformis toxicity for diverse industrial chemicals with substructure pattern recognition and machine learning methods. *Chemosphere* 2011; **82(11)**, 1636-1643.

[54] H Pajouhesh and GR Lenz. Medicinal chemical properties of successful central nervous system drugs. *NeuroRx* 2005; **2(4)**, 541-553.

[55] J Menche, A Sharma, M Kitsak, S Ghiassian, M Vidal, J Loscalzo and AL Barabási. Uncovering disease-disease relationships through the incomplete human interactome. *Science* 2015; **347(6224)**, 1257601.

[56] C Durón, Y Pan, DH Gutmann, J Hardin and A Radunskaya. Variability of betweenness centrality and its effect on identifying essential genes. *Bulletin of Mathematical Biology* 2019; **81(9)**, 3655-3673.

[57] C Liu, X Feng, Q Li and M Hua. Adiponectin, TNF-α and inflammatory cytokines and risk of type 2 diabetes: A systematic review and meta-analysis. *Cytokine* 2016; **86**, 100-109.

[58] H Alzamil. Elevated serum tnf-α is related to obesity in type 2 diabetes mellitus and is associated with glycemic control and insulin resistance. *Journal of Obesity* 2020; **2020(3)**, 5076858.

[59] C Popa, MG Netea, PLCMV Riel, JWMVD Meer and AFH Stalenhoef. The role of TNF-alpha in chronic inflammatory conditions, intermediary metabolism, and cardiovascular risk. *Journal of Lipid Research* 2007; **48(4)**, 751-762.

[60] GD Kalliolias and LB Ivashkiv. TNF biology, pathogenic mechanisms and emerging therapeutic strategies. *Nature Reviews Rheumatology* 2016; **12(1)**, 49-62.

[61] S Hussain, A Iqbal, S Hamid, PP Putra and M Ashraf. Identifying alkaline phosphatase inhibitory potential of cyclooxygenase-2 inhibitors: Insights from molecular docking, MD simulations, molecular expression analysis in MCF-7 breast cancer cell line and *in vitro* investigations. *International Journal of Biological Macromolecules* 2024; **277(P2)**, 132721.

[62] A Floegel, DO Kim, SJ Chung, SI Koo and OK Chun. Comparison of ABTS/DPPH assays to measure antioxidant capacity in popular antioxidant-rich US foods. *Journal of Food Composition and Analysis* 2011; **24(7)**, 1043-1048.

[63] R Vona, L Gambardella, C Cittadini, E Straface and D Pietraforte. Biomarkers of oxidative stress in metabolic syndrome and associated diseases. *Oxidative Medicine and Cellular Longevity* 2019; **2019**, e8267234.

[64] IR Suica-Bunghez, S Teodorescu, ID Dulama, OC Voinea, S imionescu and RM Ion. Antioxidant activity and phytochemical compounds of snake fruit (*Salacca Zalacca*). *IOP Conference Series: Materials Science and Engineering* 2016; **133(1)**, 012051.

[65] H Khotimah, SNP Alita, D Aninditha, A Weningtyas, WE Prima, U Kalsum, M Rahayu, D Handayani and SK Nandar. Ethanolic extract of Salacca zalacca peel reduce IL-1β and apoptosis in high glucose induced zebrafish embryo. *GSC Biological and Pharmaceutical Sciences* 2021; **16(03)**, 024-033.

[66] E Rohaeti, MR Fauzi and I Batubara. Inhibition of α-glucosidase, total phenolic content and flavonoid content on skin fruit and flesh extracts of some varieties of snake fruits. *IOP Conference Series Earth and Environmental Science* 2017; **58(1)**, 012066.

[67] T Ashcheulova, G Demydenko, T Ambrosova, K Kateryna, N Gerasimchuk and O Kochubiei. Carbohydrate and lipid disorders and adipokines levels in relation to body mass index in hypertensive patients. *Revista Mexicana de Cardiología* 2018; **29(2)**, 74-82.

[68] YK Denisenko, OY Kytikova, TP Novgorodtseva, MV Antonyuk, TA Gvozdenko and TA Kantur. Lipid-induced mechanisms of metabolic syndrome. *Journal of Obesity* 2020; **2020**, 5762395.

[69] O Pionova and O Kovalyova. Carbohydrate and lipid metabolism disorders in hypertensive patients with overweight and obesity PP.LB3.446. *Journal of Hypertension* 2011; **29**, e570.

[70] ND Ribatul, F Prasetya and S Badawi. Effect of Salak fruit skin tea (Salacca zalacca) on blood

glucose levels in alloxan induced mice. *Jurnal Sains dan Kesehatan* 2023; **5(1)**, 52-58.

[71] TT Liu, XT Liu, QX Chen and Y Shi. Lipase Inhibitors for Obesity: A review. *Biomedicine & Pharmacotherapy* 2020; **128**, 110314.

[72] JA Prieto-Rodríguez, KP Lévuok-Mena, JC Cardozo-Muñoz, JP Emilio, F López-Vallejo, LE Cuca and O Patino. *In vitro* and *in silico* study of the α-glucosidase and lipase inhibitory activities of chemical constituents from piper cumanense (Piperaceae) and synthetic analogs. *Plants* 2022; **11(17)**, 2188.